

See discussions, stats, and author profiles for this publication at: <https://www.researchgate.net/publication/231643384>

Resistivity Hysteresis of Ag₂S Nanocomposites

ARTICLE *in* THE JOURNAL OF PHYSICAL CHEMISTRY C · AUGUST 2007

Impact Factor: 4.77 · DOI: 10.1021/jp073814b

CITATIONS

9

READS

57

3 AUTHORS:



Sourish Banerjee

University of Calcutta

21 PUBLICATIONS 127 CITATIONS

SEE PROFILE



Santanu Bhattacharya

Mayo Foundation for Medical Education and ...

26 PUBLICATIONS 280 CITATIONS

SEE PROFILE



Dipankar Chkaravorty

Indian Association for the Cultivation of Scie...

315 PUBLICATIONS 3,603 CITATIONS

SEE PROFILE

Resistivity Hysteresis of Ag₂S Nanocomposites

Sourish Banerjee,[†] Santanu Bhattacharya,[‡] and Dipankar Chakravorty^{*‡}

Department of Physics, University of Calcutta, India, and DST Unit on Nano Science and MLS Professor's Unit, Indian Association for the Cultivation of Science, Kolkata 700032, India

Received: May 17, 2007; In Final Form: July 2, 2007

A low-temperature chemical synthesis route was used to prepare Ag₂S particles with diameters ranging from 3 to 39 nm within a silica matrix. The dc electrical resistivity was measured in the temperature range of 320–460 K. A drastic reduction in resistivity around 450 K was caused by an order–disorder transition of Ag₂S. The specimens exhibited a hysteresis in resistivity as a function of temperature. The width of the hysteresis was related to the particle size, viz., it increased with an increase in particle size. This is believed to arise due to a reduction in interfacial free energy for crystal formation in the cation sublattice for smaller Ag₂S particle sizes.

Introduction

Ag₂S has attracted a lot of attention in recent years because of its interesting properties. It is an important semiconductor with a band gap of 1 eV and has potential uses in photoconductors, photovoltaic cells, IR detectors,^{1,2} photography,³ and luminescent devices.⁴ It has been reported that Ag₂S undergoes an order–disorder transition at 450 K to an α -AgI-like body-centered cubic (bcc) lattice and the silver ions spread diffusely between tetrahedral and octahedral sites.^{5,6} Across this transition the Ag⁺ ion conductivity has been reported to increase by about 2 orders of magnitude.⁷ This has been explained as arising due to the crystallographic disorder brought about by the melting of the cation sublattice in β -Ag₂S.⁸ Nanocrystalline Ag₂S has been synthesized by chemical⁹ and gas–solid reaction¹⁰ techniques. Optical properties were measured, and it was shown that the band gap did not change appreciably from the bulk value.⁹ We have grown silver sulfide nanocrystals within a silica glass matrix and measured the electrical properties of the nanocomposite up to a temperature around 450 K. These exhibited a hysteresis in the resistivity versus temperature variation, which depended markedly on the size of the nanocrystallites. The details are reported in this paper.

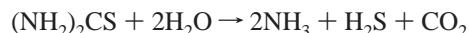
Experimental Section

Silver sulfide nanocrystallites within a silica matrix were prepared by a two-step reaction. Silver nitrate (AgNO₃), thiourea [(NH₂)₂CS], and tetraethylorthosilicate (TEOS) were used as precursors. Amounts of them were chosen to get the target composition of $x\text{Ag}_2\text{S} - (1 - x)\text{SiO}_2$ with $x = 1, 0.4$, and 0.3 . They are referred to as specimens A, B, and C, respectively. In the first step a sol was prepared with AgNO₃ and TEOS. Silver nitrate was dissolved in a mixture of ethanol and double-distilled water each taken twice the volume of TEOS. After stirring the resulting solution in a magnetic stirrer for 0.5 h, a measured volume of TEOS was added. The pH of the solution was kept at ~ 5.0 by adding 0.1 mL of 11 N nitric acid. Stirring was continued in darkness for another 2 h to get a clear sol. The sol was poured into a flat-bottomed Petri dish and kept in darkness

under ordinary atmosphere. Transparent gel pieces were obtained in the process. The resulting gel pieces were kept under vacuum of ~ 10 – 2 mbar for 1 week. Finally gel powder with composition in the system AgNO₃–SiO₂ with typical grain size of ~ 2 μm was obtained on crushing the gel pieces.

A measured amount of thiourea was dissolved in 50 mL of distilled water. Later, ammonia solution was added to the former. The pH of the solution was ~ 10 . This was slowly heated to 343 K with continuous stirring. Gel powder about a few mg was added to this solution. After stirring for a few minutes the white gel powder turned gray indicating the formation of silver sulfide phase. The process was repeated for the remaining gel powder. The resulting mixture was stirred for another 1 h at 343 K to complete the reaction. Ag₂S nanoparticles embedded in silica matrix were collected after centrifuging for 5 min at 8000 rpm. Extracted powder was washed with distilled water thoroughly to remove all unwanted materials adhering to the surface of the nanoparticles. The powder was dried at 473 K for 0.5 h.

In hot alkaline medium thiourea is hydrolyzed to yield H₂S. The reaction is as follows:



NH₃ maintains the pH of the solution, which compensates the loss due to evaporation. H₂S diffuses through the pores of silica and reacts with silver nitrate present therein. Initially, Ag₂S molecules are formed which agglomerate to nanostructure and are ultimately passivated by the silica matrix. As the nanoparticles grow within the pores of silica, the matrix itself can be used as the template as in the case of zeolite.⁴ Though silver sulfide has been referred to as Ag₂S implying a stoichiometry of Ag/S = 2:1 it should be noted that no coulometric measurements were carried out to delineate and control the value of δ in Ag_{2+ δ} S.^{11,12}

The particle sizes were measured from the micrographs taken in a JEOL 2010 transmission electron microscope (TEM) operated at 200 kV. A small amount of nanocrystalline powder was dispersed in acetone, sonicated, and placed on the carbon-coated copper grid. The crystal phases were also identified by taking X-ray diffractograms in a Rich Seifert XRD 3000P (Ahrensburg, Germany) using Cu K α radiation.

* Corresponding author. E-mail: mlsdc@iacs.res.in.

[†] University of Calcutta.

[‡] Indian Association for the Cultivation of Science.

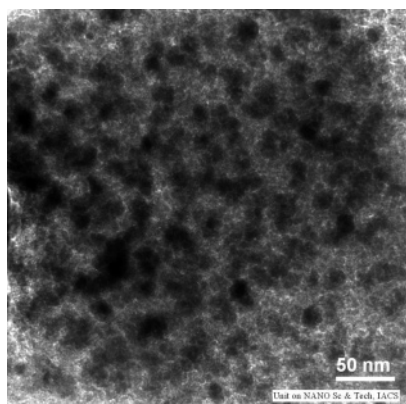


Figure 1. Transmission electron micrograph for specimen of composition 0.4Ag₂S 0.6SiO₂.

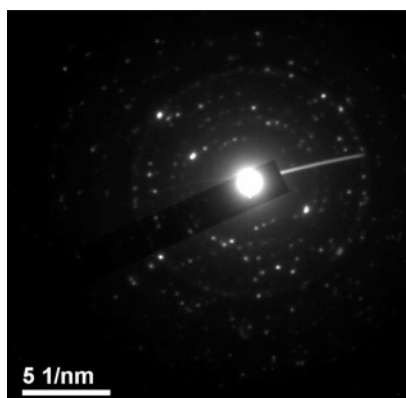


Figure 2. Electron diffraction pattern obtained from Figure 1.

TABLE 1: Comparison of Interplanar Spacings Obtained from Specimen with ASTM Values (14-0072)

obsd d_{hkl} (nm) from TEM diff	obsd d_{hkl} (nm) from X-ray diff	ASTM silver sulfide (nm)
0.340	0.343	0.3437
0.308	0.308	0.308
0.280	0.283	0.2836
0.261	0.260	0.2606
0.236	0.238	0.2383
0.226	0.222	0.2213
	0.208	0.2083
	0.199	0.1995
	0.1962	0.1963
0.193		0.1935
0.172	0.172	0.1718

Pellets of area ~ 0.7 cm² and thickness ~ 1 mm were prepared for electrical characterization. A small amount of nanocomposite powder was cold pressed by applying pressure of 2.5 ton/cm² for 10 min. The two opposite faces of the pellets were coated with silver paint electrodes supplied by Acheson Colloiden B. V. Holland. Electrical measurements were carried out by a Keithley 6514 system electrometer over the temperature range of 300–460 K. The temperature of the chamber was controlled by a Eurotherm model 3216 temperature controller. Temperature versus resistance data in both heating and cooling cycles were collected in computer by standard serial and GPIB interfacing method.

Results and Discussion

Figure 1 is the transmission electron micrograph for the specimen B. Figure 2 is the selected area electron diffraction pattern obtained from Figure 1. Table 1 shows a comparison between the interplanar spacings d_{hkl} obtained from the diameters

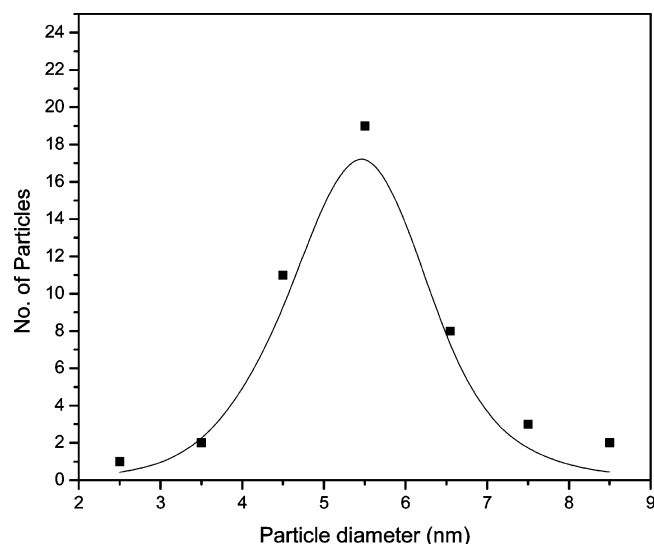


Figure 3. Histogram of Ag₂S particle sizes from Figure 1.

TABLE 2: Ag₂S Particle Sizes Obtained from Electron Micrograph and X-ray Diffraction Line Broadening

specimen	TEM		particle size from X-ray line broadening (nm)
	median diameter (nm)	geometric standard deviation	
A			23.3
B	6	1.2	13.9
C	4.5	1.3	10.3

of the diffraction rings in Figure 2 and the standard data [JCPDS 14-0072] for Ag₂S. There is a good agreement between these two sets of values.

Figure 3 shows the histogram of Ag₂S particle sizes as obtained from Figure 1. The experimental points in this figure were fitted to a log-normal distribution function. The median diameter \bar{x} and geometric standard deviation σ for all the specimens were calculated. These values are summarized in Table 2. It is seen that the size of the Ag₂S nanoparticles can be controlled by changing the precursor concentration of silver nitrate and thiourea.

Figure 4 gives the X-ray diffraction profiles for all the specimens. The d_{hkl} values are indicated on the peak positions in the figure. The typical interplanar spacings d_{hkl} as obtained from the diffraction peaks are compared with standard ASTM values for Ag₂S in Table 1. The phase of the silver sulfide is confirmed to be achantite (α -Ag₂S) with monoclinic symmetry from ASTM data.

The crystallite size was estimated from the broadening of the diffraction line using the Scherrer equation.¹³ Estimated particle diameters are shown in Table 2. The particle sizes as obtained from TEM studies are smaller than those derived by X-ray analysis. This could be due to agglomeration of particles.

Figure 5a–c shows the variation of logarithm of dc resistivity as a function of temperature for specimens A, B, and C, respectively. In each plot the data of heating and cooling cycles are indicated by arrows. The resistivity values are consistently increased for the reduction of particle size. All the specimens show a decreasing trend of resistivity with increasing temperature. The effect is pronounced at some higher temperature where resistivity changes by about 2 orders of magnitude by a slight change in temperature. This is the transition temperature associated with the transition of silver sulfide from its low-temperature α -phase (achantite) to high-temperature β -phase (argentine).

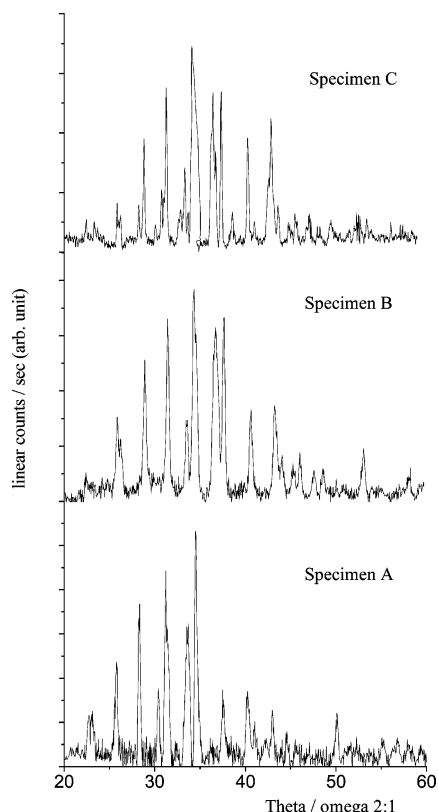


Figure 4. X-ray diffractogram of different specimens.

We have estimated the transition points for the three specimens. These are listed in Table 3. A remarkable shift in transition temperature is observed with the reduction of particle size. For specimen A, SiO_2 matrix is absent and the particle size is the largest with a transition temperature close to 450 K.

Silver sulfide exhibits an order–disorder transition at 450 K.¹² The high-temperature disordered phase has a high Ag-ion conductivity just as in the high-temperature phase of AgI. This order–disorder transition has often been described in terms of melting of the silver sublattice. In the high-temperature superionic $\beta\text{-Ag}_2\text{S}$ phase, the S sublattice is ordered in a bcc lattice, while the four Ag ions in the unit cell are distributed among the tetrahedrally and octahedrally coordinated positions. The occupancy ratio is about 3:1 just above the transition temperature, at higher temperatures the tetrahedral occupancy increases at the expense of the octahedral occupancy, and above 533 K the occupied sites are entirely tetrahedral. This fact is confirmed by neutron diffraction study.⁶

The salient feature of the present study is the resistivity hysteresis observed in heating and cooling cycles. The samples remain at the low-resistance state in the cooling cycle even when the temperature is sufficiently low. Repeated measurements have shown that both magnitudes of resistivity and transition temperatures were reproducible to within $\pm 2\%$. Also, there was no effect of heating or cooling rate on the observed hysteresis. The plots indicate that the effect of hysteresis is weak for smaller particle size. The temperature hysteresis values are shown in the Table 3.

Silver ions in the molten sublattice are equivalent to the ions distributed in a glassy phase with high degree of disorder. Here silver ions in the tetrahedral and octahedral sites are distributed in random fashion though the overall structure has cubic symmetry above the transition temperature. The ordered structure below the transition temperature can be visualized to be due to a liquid to crystal transition. The latter takes place by a

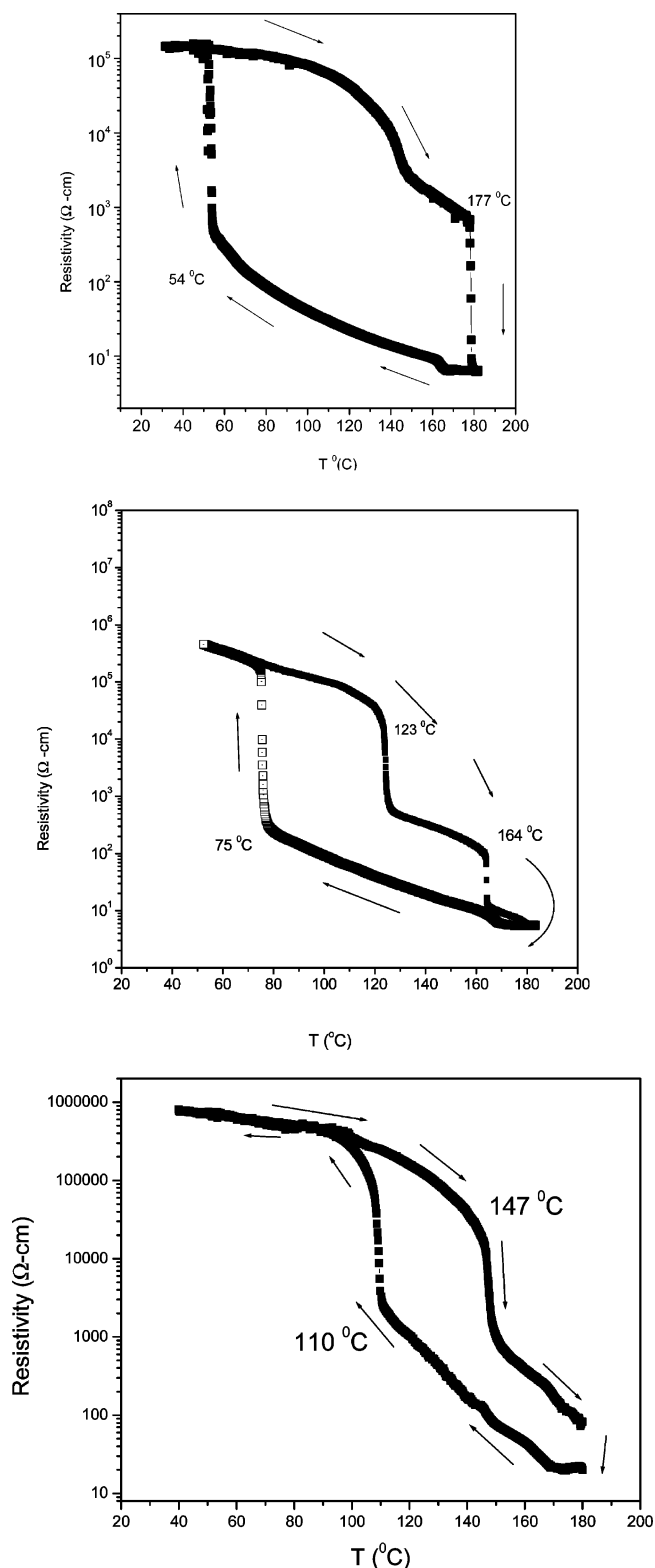


Figure 5. Logarithm of dc resistivity as a function of temperature for different specimens: (a) specimen A; (b) specimen B; (c) specimen C.

nucleation and growth process.¹⁴ The activation barrier ΔG for the critical nuclei of the crystalline phase (in the cation sublattice) is related to the interfacial free energy γ and the undercooling ΔT below the transition temperature by¹⁴

$$\Delta G \propto \frac{\gamma^3}{(\Delta T)^2} \quad (1)$$

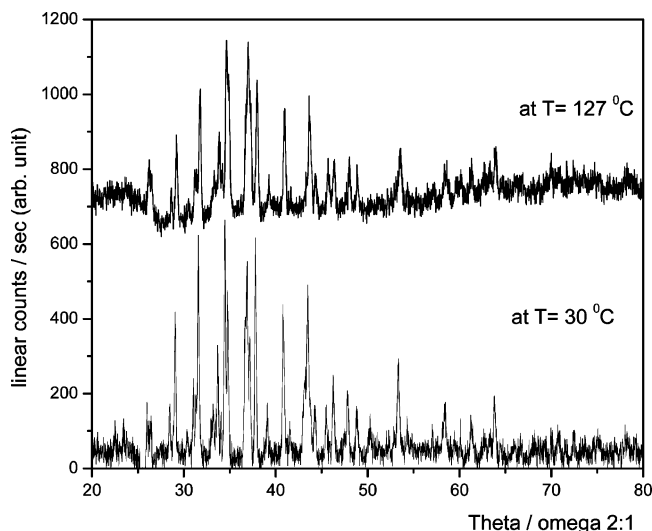
TABLE 3: Transition Temperature and Resistivity Hysteresis in Different Specimens

specimen no.	particle size (nm)	transition temperature (K)	degree of hysteresis (K)
A large	23.3	450	123
B	13.9	437	89
C smallest	10.3	453	70

It should be evident from eq 1 that the rate of reaction for the nuclei formation will depend on both γ and ΔT . For smaller particle sizes with diameters of the order of nanometers the interfacial energy γ for crystal formation should also be smaller. As a result, to achieve a certain amount of the relevant phase transformation the extent of undercooling needed will be small. This is borne out by the data summarized in Table 3.

The staircase behavior in the resistivity temperature plots below 450 K is ascribed to a phase transition which was confirmed by taking in situ X-ray diffractograms of the specimen at a temperature slightly lower than the discontinuity. A PANalytical X'PERT PRO diffractometer was used for this purpose. Figure 6 shows the X-ray diffractogram of specimen C at 400 K. Also shown in this figure is the X-ray pattern obtained from specimen C at 303 K for comparison. The interplaner spacings of the 400 K pattern were analyzed by the software program TREOR.¹⁵ The latter indicated the presence of both a monoclinic and an orthorhombic phase. The latter has unit cell parameters as follows: $a = 3.2$ Å; $b = 9.6$ Å; $c = 12.2$ Å; $\alpha = \gamma = \beta = 90^\circ$. Evidently, the orthorhombic phase enhances the mobility of silver ions, and the conductivity shows a discontinuous increase at a temperature of 420 K (see Figure 5c).

It should be mentioned that so far we have not discussed the possibility of silver nanoparticle diffusion within the sample under the influence of an applied electric field used for dc resistivity measurements. The voltage applied across the specimen by the Keithley electrometer for resistance measurement is of the order of a few millivolts. It has been shown earlier that arrays of silver nanoparticles can be grown within a glass containing silver ions by the application of at least 10 V at a temperature around 475 K.^{16,17} The latter is an electrodeposition process and does not involve any diffusion of silver nanoparticles as such. Also, the voltage needed for such growth of nanostructure is a few orders of magnitude higher than that used for dc resistance measurement in the present case. Even if such

**Figure 6.** X-ray diffractogram of specimen C at 400 and 303 K.

a microstructure were induced within the sample there would be no hysteresis effect as observed here. Last, a microstructure involving nanowires of silver formed by the interconnection of silver nanoparticles would show a temperature variation of resistance with an opposite trend to that exhibited by the present set of samples. On the basis of these considerations the effect of silver paste on the resistivity hysteresis can be ruled out.

There have been quite a few publications in the literature on the synthesis of silver sulfide and its structure. Also, the resistivity change at 450 K has been ascribed to an order–disorder transition involving melting of the silver ion sublattice. The present investigation gives the first direct evidence of this type of unusual transition, viz., melting of a particular sublattice. The hysteresis effect clearly is consistent with the theory of phase transformation describing a crystal to liquid transition.

Conclusions

In summary, nanocomposites of Ag₂S in a silica glass matrix have been synthesized and their dc electrical resistances have been investigated. The order–disorder transition at around 450 K has been observed in terms of a drastic decrease in resistivity. A resistivity hysteresis as a function of temperature has been recorded. The hysteresis is reduced as the Ag₂S particle size becomes smaller. This has been explained as occurring due to a decrease in the interfacial free energy needed to form nuclei of the crystalline phase in the cation sublattice as the particle size is reduced.

Acknowledgment. S. Bhattacharya thanks C.S.I.R., New Delhi for the award of a Senior Research Fellowship. D. Chakravorty thanks I.N.S.A, New Delhi for the award of a Senior Scientist position. The work was supported by DST, New Delhi under its Nano Science and Technology Initiative Programme. The experimental help extended by Debnath Sadhukhan is gratefully acknowledged.

References and Notes

- (1) Kitova, S.; Eneva, J.; Panov, A.; Haefke, H. *J. Imaging Sci. Technol.* **1994**, *38*, 484.
- (2) Hodes, G.; Manasen, J.; Cahen, D. *Nature* **1976**, *261*, 403.
- (3) Baetzold, R. C. *J. Imaging Sci. Technol.* **1999**, *43*, 375.
- (4) Bruhwiler, D.; Leiggenger, C.; Glans, S.; Calzaferri, G. *J. Phys. Chem. B* **2002**, *106*, 3770.
- (5) Cava, R. J.; McWhan, D. B. *Phys. Rev. Lett.* **1980**, *48*, 2046.
- (6) Cava, R. J.; Reidinger, F.; Wuensch, B. J. *J. Solid State Chem.* **1980**, *31*, 69.
- (7) Vasan, H. N.; Shukla, A. K. *Bull. Mater. Sci.* **1981**, *3*, 399.
- (8) Junod, P.; Hediger, H.; Kilchor, B.; Wulschleger, J. *Philos. Mag.* **1977**, *36*, 941.
- (9) Schaaff, T. G.; Rodinone, A. J. *J. Phys. Chem. B* **2003**, *107*, 10416.
- (10) Wen, X.; Wang, S.; Xie, Y.; Li, X. Y.; Yang, S. *J. Phys. Chem. B* **2005**, *109*, 10100.
- (11) Shukla, A. K.; Schmalzried, H. Z. *Phys. Chem. Neue Folge* **1979**, *118*, 59.
- (12) Barman, S. R.; Shanthi, N.; Shukla, A. K.; Sarma, D. D. *Phys. Rev. B* **1996**, *53*, 3746.
- (13) Klug, H. P.; Alexander, L. E. *X-ray Diffraction Procedures for Polycrystalline and Amorphous Materials*, 2nd ed.; Wiley-Interscience: New York, 1974; p 689.
- (14) Roduner, E. *Nanoscope Materials*; Royal Society of Chemistry Publication, 2006; p 136.
- (15) Werner P. E. *TREOR, a Trial and Error Programme for Indexing Unknown Powder Patterns*; University of Stockholm: Stockholm, Sweden, 1984.
- (16) Roy, S.; Chakravorty, D. *Phys. Rev. B* **1993**, *47*, 3746.
- (17) Dan, A.; Satpati, B.; Satyam, P. V.; Chakravorty, D. *J. Appl. Phys.* **2003**, *93*, 4794.